

Valence Instability and Superconductivity in Heavy Fermion Systems

Alexander T. HOLMES^{1*}, Didier JACCARD² and Kazumasa MIYAKE³

¹*KYOKUGEN, Center for Quantum Science and Technology under Extreme Conditions, Osaka University, Toyonaka, Osaka 560-8531*

²*Département de Physique de la Matière Condensée, Section de Physique, University of Geneva, 24 quai Ernest-Ansermet CH-1211 Genève 4, Switzerland*

³*Department of Materials Engineering Science, Graduate School of Engineering Science, Osaka University, Toyonaka, Osaka 560-8531*

Many cerium-based heavy fermion (HF) compounds have pressure-temperature phase diagrams in which a superconducting region extends far from a magnetic quantum critical point. In at least two compounds, CeCu₂Si₂ and CeCu₂Ge₂, an enhancement of the superconducting transition temperature was found to coincide with an abrupt valence change, with strong circumstantial evidence for pairing mediated by critical valence, or charge transfer, fluctuations. This pairing mechanism, and the valence instability, is a consequence of a $f - c$ Coulomb repulsion term U_{fc} in the hamiltonian. While some non-superconducting Ce compounds show a clear first order valence instability, analogous to the Ce $\alpha - \gamma$ transition, we argue that a weakly first order valence transition may be a general feature of Ce-based HF systems, and both magnetic and critical valence fluctuations may be responsible for the superconductivity in these systems.

KEYWORDS: heavy fermion superconductors, mixed valence compounds, CeCu₂Si₂, CeCu₂Ge₂, superconductivity, fluctuations in superconductors, critical valence fluctuations, new paradigm

1. Introduction

A resurgence of interest in heavy fermion (HF) superconductivity in the last few years has been strongly driven by the discovery of a large number of new Ce and U based intermetallic superconductors. Most analyses of their behaviour have focused on the relationship between superconductivity and magnetism, specifically on the idea that superconductivity in these systems is mediated by low energy magnetic fluctuations around a so-called magnetic quantum critical point (QCP), where a magnetic ordering temperature is driven to zero by an external parameter such as pressure or chemical substitution.

The aim of this article is to draw attention to another phenomenon in Ce compounds, namely a weakly first order valence instability also capable of generating superconductivity. In this case the pairing is mediated by the exchange of critical valence, or charge-transfer, fluctuations (CVF).¹⁾ It is the view of the authors that this scenario is of widespread importance, and must be taken into account for a complete understanding of the behaviour of all Ce-based HF compounds. We emphasise the heavy fermion nature of these superconductors; those Ce compounds in which the f-electrons play little role in their superconductivity do not concern us for the purposes of this discussion.

We will start by a brief description of the superconducting pressure-temperature phase diagram of all known Ce-based HF superconductors, followed by a discussion of the first order valence transition found in pure Cerium and a few other of its compounds. After reviewing the theoretical basis for CVF-mediated supercon-

ductivity, we will look at one compound in particular, CeCu₂Si₂, and show that there is very strong evidence for such a mechanism in this system, and in its isoelectronic sister compound CeCu₂Ge₂. Finally, we will discuss to what extent there is evidence for similar behaviour in other compounds.

2. Pea versus Potato

We can divide Ce-based HF superconductors into two categories, characterised by the shape of their superconducting region in the pressure-temperature phase diagram. We will call these two categories ‘pea’ and ‘potato’ (Fig. 1).

The first category contains those which show a small dome of superconductivity, typically with a pressure width of less than or equal to 1 GPa, symmetrically situated around the pressure P_c where the Néel temperature T_N tends to zero. This type of phase diagram is expected in a spin fluctuation mediated scenario, where the spin susceptibility diverges at the critical pressure P_c , and the coherence length ξ of the Cooper pairs increases with $|P - P_c|$. When ξ is less than the mean free path ℓ , superconductivity can occur, leading to a dome-shaped superconducting region around P_c (small and round, like a pea).

In the second category, the ‘potatoes’, are compounds whose superconducting pressure domains are much less regularly shaped, typically having a higher maximum T_c , which may not be situated exactly at P_c . Superconductivity in these compounds can be found over a much broader pressure range than in the previous category, often extending far from P_c .

Table I shows the classification of the known Ce-based HF superconductors for which sufficient data un-

*E-mail address: alex@djebel.mp.es.osaka-u.ac.jp

Table I. Classification of Ce-based HF superconductors as indicated in text. Compounds marked * show traces of superconductivity. N.b. there is insufficient pressure data to classify $\text{Ce}_2\text{Ni}_3\text{Ge}_5$ and Ce_2CoIn_8 .

| 'Pea' | | 'Potato' | | |
|---|--|--|---|---|
| CeIn_3 , ⁷⁾ | CePd_2Si_2 , ⁷⁾ | CeCu_2Si_2 , ⁸⁾ | CeCu_2Ge_2 , ⁹⁾ | CeNi_2Ge_2 , ¹⁰⁾ |
| CeRh_2Si_2 , ¹¹⁾ | CeCu_5Au * ¹²⁾ | CeCoIn_5 , ¹³⁾ | CeRhIn_5 , ¹⁴⁾ | CeIrIn_5 , ¹⁴⁾ |
| CeCu_2 * ¹⁵⁾ | | | Ce_2RhIn_8 , ¹⁶⁾ | CeNiGe_3 , ¹⁷⁾ |
| | | | CePt_3Si , ¹⁸⁾ | CeRhSi_3 , ¹⁹⁾ |
| | | | | CeIrSi_3 , ²⁰⁾ |

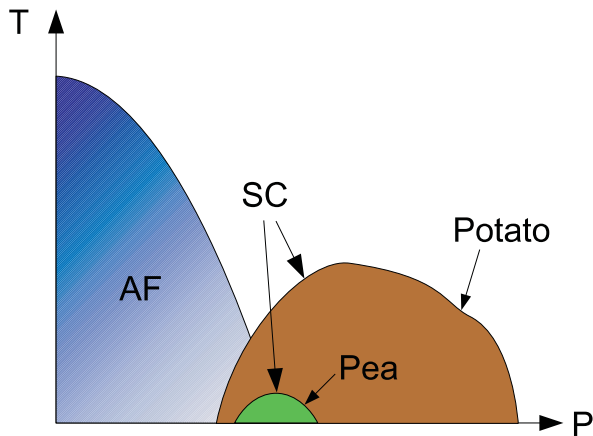


Fig. 1. Schematic pressure-temperature phase diagrams of two classes of Ce-based HF superconductors. The ‘peas’ have a small pocket of superconductivity centred on P_c (where $T_N \rightarrow 0$), while the ‘potatoes’ have a large and asymmetrical superconducting region.

der pressure exist. Remarkably enough, the ‘potatoes’ outnumber the ‘peas’ by quite a considerable margin. The phase diagrams were mostly determined by resistivity. In CePd_2Si_2 for example, bulk superconductivity was found by specific heat measurements only at exactly P_c .²⁾

In the spin-fluctuation scenario, the scale of T_c is set by the characteristic spin-fluctuation temperature T_{sf} . In addition, it has been suggested with respect to the Ce115 compounds CeCoIn_5 , CeRhIn_5 , and CeIrIn_5 , that the enhancement of T_c compared to CeIn_3 is due to the quasi-two dimensional character of these compounds.³⁻⁵⁾ Considerations of dimensionality are almost certainly very important, but they do not resolve the question of the nature of the pairing mechanism, since the effect applies both to magnetic and density fluctuation mediated superconductivity.⁶⁾

We emphasise again that in seeking an explanation for the irregularly shaped superconducting regions found in the majority of Cerium-based HF superconductors, magnetic fluctuations and dimensionality are not the only items on the menu. Before considering a purely magnetic scenario, one must at least rule out the influence of critical valence fluctuations.

3. Local versus Itinerant Cerium f Electron

The behaviour of Ce and its compounds is dominated by its single 4f electron. It is rather loosely bound, and can easily be promoted into the conduction band leav-

ing a non-magnetic Ce^{4+} ion, which has a smaller ionic radius than the Ce^{3+} ion. Pressure therefore tends to favour a Ce^{4+} configuration.

In the Ce^{3+} (trivalent) state the f electron is localised and carries a magnetic moment, which can order magnetically, or be screened by conduction electrons via the Kondo effect. In the trivalent state, pressure increases the coupling J between the f and conduction electrons, which tends both to promote the formation of a Kondo-Yosida singlet, and to encourage magnetic ordering via the RKKY effect. The Kondo effect increases more rapidly with J , so the overall effect is for magnetic order to be eventually suppressed, leading to the aforementioned magnetic QCP where the ordering temperature reaches zero.

Ce compounds at a given pressure can be classified by the nature of the f-electron into two categories, often referred to as the Kondo and valence fluctuation regimes respectively:

- (1) Ce^{3+} , $4f^1$ localised. Magnetic moment possibly ordered and/or (partially) screened by Kondo effect. Kondo temperature $T_K \sim 10\text{K}$. Properties corresponding to a strongly correlated electron system. Kadowaki-Woods ratio²¹⁾ $A/\gamma^2 \simeq 10^{-5} [\mu\Omega\text{cm mol}^2\text{K}^2/\text{J}^2]$.
- (2) $\text{Ce}^{(3+\delta)+}$, $4f^1 \rightleftharpoons 4f^0 + [5d6s]$, itinerant. T_K larger than or comparable to crystalline electric field (CEF) splitting. No magnetic order. Intermediate valence. Kadowaki-Woods ratio $A/\gamma^2 \simeq 0.4 \times 10^{-6} [\mu\Omega\text{cm mol}^2\text{K}^2/\text{J}^2]$.

3.1 Ce $\alpha - \gamma$ transition

Cerium metal is well known for the first-order isostructural volume discontinuity, known as the $\alpha - \gamma$ transition, in its pressure-temperature phase diagram. This corresponds to a delocalisation of the Ce 4f electron, as described above. In pure Ce, the transition itself is strongly first order, with a large hysteresis, and a critical end point at rather high temperature, around 600 K and 20 kbar, with a large experimental uncertainty due to the nature of the transition.²²⁾

3.2 First order transition in cerium compounds

There are a small number of Ce compounds which also show a first order valence transition, including CeNi ,²³⁾ CeP ,²⁴⁾ $\text{Ce}_{0.74}\text{Th}_{0.26}$ ²⁵⁾ $\text{Ce}(\text{Rh}_{0.69}\text{Ir}_{0.31})\text{Ge}$.²⁶⁾ See also ref. 27 and refs therein for a discussion of first order transitions in Ce, Yb and Eu chalcogenides and pnictides.

These compounds are all notable for containing a high atomic percentage of Ce, and hence a small Ce-Ce interatomic separation. None of them display heavy fermion superconductivity.

4. Theory of Valence Transition and Critical-Valence-Fluctuation Mediated Superconductivity

The idea of CVF-mediated superconductivity and related anomalous phenomena can be backed up by a microscopic calculations on the basis of a generalized periodic Anderson model (GPAM):¹⁾

$$\begin{aligned}
 H_{\text{GPAM}} = & \sum_{k\sigma} (\epsilon_k - \mu) c_{k\sigma}^\dagger c_{k\sigma} + \varepsilon_f \sum_{k\sigma} f_{k\sigma}^\dagger f_{k\sigma} \\
 & + V \sum_{k\sigma} (c_{k\sigma}^\dagger f_{k\sigma} + \text{h.c.}) + U_{\text{ff}} \sum_i n_{i\uparrow}^f n_{i\downarrow}^f \\
 & + U_{\text{fc}} \sum_{i\sigma\sigma'} n_{i\sigma}^f n_{i\sigma'}^c, \quad (1)
 \end{aligned}$$

where notations are conventional except for U_{fc} , the local Coulomb repulsion between f- and conduction electrons, which is a crucial ingredient for a sharp valence transition.

4.1 Critical-valence-fluctuation mediated superconductivity

In ref. 1, the model Hamiltonian (1) with a spherical conduction band (i.e., $\epsilon_k = k^2/2m - D$, where D is the Fermi energy of conduction electrons if it were decoupled from f-electrons) was treated by the mean-field (MF) approximation in the slave bosons formalism (with $U_{\text{ff}} \rightarrow \infty$) to discuss the possibility of valence transition, and by the Gaussian fluctuation theory around the mean-field solution to discuss a possible superconducting state. As shown in Fig. 2, the central results of ref. 1 are summarized as follows:

- 1) Sharp valence change is caused by the effect of U_{fc} with moderate strength, of the order of the Fermi energy (D) of conduction electrons, when the f-level ϵ_f is tuned to mimic the effect of the pressure.
- 2) The superconducting state is induced by the process of exchanging slave-boson fluctuations for the values of ϵ_f around which the sharp valence change occurs.
- 3) The symmetry of the induced superconducting state is *d*-wave if a spherical model is adopted for conduction electron. However, as seen in the argument below, anisotropic pairing is induced by the CVF modes due to their *almost local* nature.

The peak of T_c occurs at ϵ_f slightly smaller than that corresponding to the steepest slope of \bar{n}_f vs ϵ_f relation, where \bar{n}_f denotes f-electron number per site and “spin”. Since ϵ_f simulates the pressure variation, this aspect of the pressure dependence of T_c reproduces well that observed experimentally in CeCu₂Ge₂ under pressure.⁹⁾ It is also remarked that a sharp change of \bar{n}_f is related to that of the mass enhancement m^*/m by a canonical relation in strongly correlated limit:^{28,29)}

$$\frac{m^*}{m} = \frac{1 - \bar{n}_f}{1 - 2\bar{n}_f}, \quad (2)$$

which in turn implies a drastic decrease of the coefficient of the T^2 -term of the resistivity A , because A is proportional to $\gamma^2 \propto (m^*/m)^2$.^{21,30)}

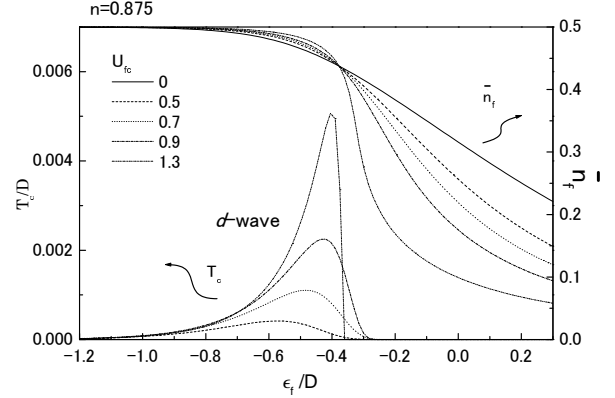


Fig. 2. T_c for the *d*-wave channel and \bar{n}_f , f-electron number per site and “spin”, as a function of ϵ_f . The total number of electrons per site and “spin” is set as $n = 0.875$, and the c-f hybridization is set as $V = 0.5D$. The unit of energy is given by D , the Fermi energy of parabolic conduction band if it were decoupled from f-electrons: the dispersion $\epsilon_k = k^2/2m - D$ is adopted for the conduction electrons.

The ϵ_f -dependence of \bar{n}_f is smooth without U_{fc} , while its dependence becomes steep as U_{fc}/D is increased to a moderate strength of $\mathcal{O}(1)$. These results are consistent with a physical picture that the rapid valence change occurs at the condition $\epsilon_f + U_{\text{fc}}n_c \approx E_F$ (the Fermi energy of the f^0 -state) where the energy of the f^0 - and f^1 -state are degenerate, leading to enhanced valence fluctuations. For much larger values of U_{fc}/D or smaller values of V than those presented in Fig. 2, there occurs a first-order like discontinuous transitions although they are not shown here. However, the valence change occurs more sharply if we treat the problem in much more proper approximation on the extended Gutzwiller variational wave function.³¹⁾

It is remarked that T_c can exist only for the *d*-wave ($\ell = 2$) channel as far as the channels, $\ell = 0, 1$ and 2 , are concerned. There exists a sharp peak of T_c at around ϵ_f where \bar{n}_f starts to show a rapid decrease. Its tendency becomes more drastic as U_{fc}/D increases, making the valence change sharper. In the region where the f-electron number \bar{n}_f is decreased enough, T_c is strongly suppressed. This suggests that the CVF associated with the sharp valence change of Ce ions is the origin of the pairing.

The pairing interaction $\Gamma^0(q)$ ($= V_{\mathbf{k},\mathbf{k}'}$ with $\mathbf{q} = \mathbf{k} - \mathbf{k}'$) is calculated by taking into account the Gaussian fluctuations of slave bosons around the MF solution as mentioned above. The result is shown in Fig. 3 for the parameter set $\varepsilon = -0.5D$ and $U_{\text{fc}} = 0.9D$.¹⁾ One can see clearly that the scattering process (f,f) \rightarrow (f,c) or (f,c) \rightarrow (f,f), in which the valence of f-electrons is changed, plays a dominant role. It is also remarked that $\Gamma^0(q)$ is almost q -independent up to $q \simeq (3/2)k_F$, reflecting the *local* nature of the valence transition.

The reason why *d*-wave pairing can be realized is understood in the following way. While $\Gamma^0(q)$ is always

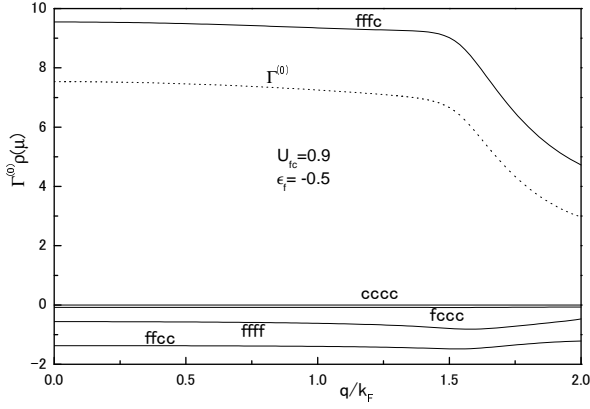


Fig. 3. Pairing interaction $\Gamma^0(q)\rho(q)$, $\rho(q)$ being the quasiparticle density of states at the Fermi level.

positive and almost constant at $0 < q < (3/2)k_F$, giving a short-range strong repulsion, the sharp decrease at $q > (3/2)k_F$ gives an extended attraction, leading to pairing of non-zero angular momentum, such as $\ell = 1$ and 2. One can see this more vividly by inspecting a real space picture of the pairing interaction

$$\Gamma^0(r) = \sum_{\mathbf{q}} \Gamma^0(q) e^{i\mathbf{q}\cdot\mathbf{r}}. \quad (3)$$

The result for $\Gamma^0(r)$ is shown in Fig. 4 for the same parameter set as Fig. 3. This clearly shows an existence of the extended attraction together with the on-site strong repulsion. If we assume $k_F \sim \pi/a$, a being the lattice constant as in typical metals, the attraction works between nearest neighbor sites. Then, according to the discussion in ref. 32, pairing of d -wave symmetry is promoted. Pairing with p -wave symmetry is also possible in principle in this case because the attraction mediated by the valence fluctuation has no spin dependence.

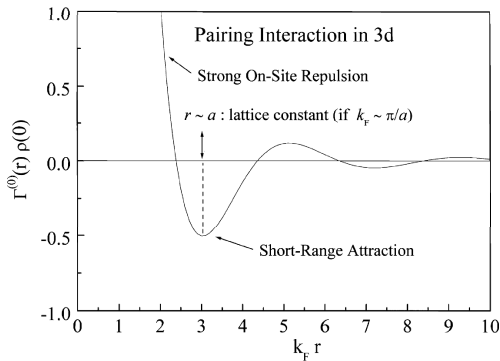


Fig. 4. Real-space pairing interaction $\Gamma^0(r)\rho(0)$. The parameter set adopted is the same as Fig. 3.

Quite recently, Watanabe *et al.*³³ reported results on the density-matrix-renormalisation-group analysis for the one-dimensional (1d) version of the model Hamilto-

nian (1) in which the conduction band is given as

$$\epsilon_k = -t \sum_{i\sigma} (c_{i\sigma}^\dagger c_{i+1\sigma} + c_{i+1\sigma}^\dagger c_{i\sigma}), \quad (4)$$

where t is the nearest-neighbour hopping integral. For an electron number $7/4$ per site, $V/t = 0.1$ and $U/t = 100$, a first order valence-transition line in $U_{fc}-\epsilon_f$ plane has been determined, showing that the region of uniform phase is stabilized and phase separation is suppressed due to quantum fluctuations. By analysis of the exponent of the long-range behaviour of correlation functions of inter-site pairing, it has been shown that superconducting correlations become dominant against charge and spin density wave correlations near the QCP of the valence transition in the region of uniform phase. This result supports the overall picture of CVF-mediated unconventional superconductivity discussed in ref. 1.

4.2 T -linear resistivity and enhanced Sommerfeld coefficient

Here we briefly discuss how a critical behavior of the resistivity and the specific heat arises around the critical valence transition at $P = P_v$. The local nature of the pairing interaction can be seen also in the CVF spectrum. By exploiting this nature, the valence fluctuation propagator χ_v (dynamical valence susceptibility) may be parameterized as

$$\begin{aligned} \chi_v(q, \omega) &\equiv i \int_0^\infty dt e^{i\omega t} \langle [n_f(q, t), n_f(-q, 0)] \rangle \quad (5) \\ &= \frac{K}{\omega_v - i\omega}, \quad \text{for } q < q_c \sim p_F \quad (6) \end{aligned}$$

where $n_f(q)$ is the Fourier component of the number of f -electrons per Ce site, and the parameter ω_v parameterizes the closeness to criticality. ω_v is inversely proportional to the valence susceptibility $\chi_v(0, 0) = -(\partial n_f / \partial \epsilon_f)_\mu$.

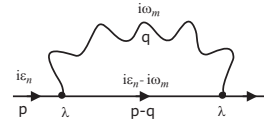


Fig. 5. Feynman diagram for the self-energy due to one-fluctuation mode exchange process. λ denotes the coupling between the valence-fluctuation mode and the quasiparticles.

With the use of the propagator (6), it is a straightforward calculation to obtain a self-energy $\Sigma_{vf}^R(p, \epsilon + i\delta)$ of quasiparticle due to one CVF exchange process shown in Fig. 4.2. It is reduced to simple forms in typical limiting cases as follows:

In the case $\epsilon = 0$, $0 < T \ll \epsilon_F$, ϵ_F being the effective quasiparticle Fermi energy,

$$\text{Im}\Sigma_{vf}^R(p_F, 0) \simeq -\frac{|\lambda|^2 K q_c^2}{4\pi^2 v} \begin{cases} \left(\frac{T}{\omega_v}\right)^2, & T \ll \omega_v, \\ \frac{\pi T}{2\omega_v}, & T \gg \omega_v, \end{cases} \quad (7)$$

where p_F is the Fermi momentum, and in the case $T = 0$ and $\epsilon \sim 0$,

$$\begin{aligned} \text{Re}\Sigma_{\text{vf}}^{\text{R}}(p_F, \epsilon) &\simeq -\frac{|\lambda|^2 K q_c^2}{2\pi^2 v_F} \frac{\epsilon}{\omega_v} \int_0^1 du \frac{1-u^2}{u^2+1} \ln \left| \frac{1}{u} \right| \\ &\propto -\frac{\epsilon_F}{\omega_v} \epsilon, \end{aligned} \quad (8)$$

where v_F is the Fermi velocity of quasiparticles, and $K \sim \epsilon_F \rho(0)$ has been used.

The result of eq. (7) for $T \gg \omega_v$ implies that almost all the critical valence-fluctuation modes can be regarded as classical at $T > \omega_v$, leading to the T -linear resistivity, because the quasiparticles are subject to large angle scattering by the CVF modes which are effective in a wide region in the Brillouin zone through the Umklapp process.

Moreover, eq. (8) implies that an extra enhancement of the Sommerfeld coefficient is expected other than that of quasiparticles. Namely, $\gamma/\bar{\gamma} \propto \epsilon_F/\omega_v$ where $\bar{\gamma}$ is the Sommerfeld coefficient enhanced by the local correlation given by eq. (2). $\bar{\gamma}$ is a sharply decreasing function of the pressure (or ϵ_f) around $P = P_v$ while a factor $1/\omega_v$ has a sharp peak at $P = P_v$. Then the resultant γ at low temperature should exhibit a sharp structure around $P = P_v$.

4.3 Enhanced residual resistivity

The CVF can give rise to huge enhancement of the residual resistivity ρ_0 at around $P \sim P_v$ through a many-body effect on the impurity potential. In the forward scattering limit, this enhancement is proportional to the valence susceptibility $-(\partial n_f/\partial \epsilon_f)_\mu$, where ϵ_f is the atomic f-level of the Ce ion, and μ is the chemical potential.³⁴⁾ Physically speaking, local valence change coupled to the impurity or disorder gives rise to the change of valence in a wide region around the impurity which then scatters the quasiparticles quite strongly, leading to the increase of ρ_0 (see Fig. 6). Thus the enhancement of ρ_0 can be directly related to the degree of sharpness of the valence change because the variation of the atomic level ϵ_f is considered to be a smooth function of the pressure. The critical pressure P_v is indeed defined by the maximum of ρ_0 .

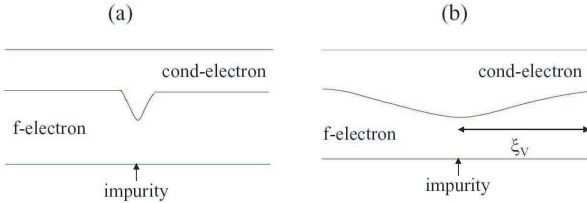


Fig. 6. Schematic view of charge distribution of f- and conduction electrons around impurity: (a) at far from $P \sim P_v$ where the effect of impurity remains as short-ranged so that the residual resistivity ρ_0 is not enhanced; (b) at around $P \sim P_v$ where the effect of impurity extends to long-range region, because the correlation length ξ_v of valence fluctuations diverges as $P \rightarrow P_v$, leading to highly enhanced ρ_0 .

It is remarked that there are two kinds of impurity potential for quasiparticles consisting mainly of f-electrons: One is due to the disorder of non-f elements and another is due to the defect of Ce ions. The former gives essentially the Born scattering, while the latter causes the scattering in the unitarity limit. Then the residual resistivity is expressed as

$$\rho_0 = \rho_0^{\text{Born}} + \rho_0^{\text{unit}}, \quad (9)$$

where ρ_0^{Born} is subject to huge enhancement by the CVF and ρ_0^{unit} is essentially unaffected. Then, eq. (9) is expressed as

$$\rho_0 = B c_{\text{imp}} |u(0)|^2 \ln \left| \left(-\frac{\partial n_f}{\partial \epsilon_f} \right)_\mu \right| / N_F + \rho_0^{\text{unit}} \quad (10)$$

where c_{imp} is the concentration of impurities with scattering potential $u(q)$, and the coefficient B depends on the band structure of the host metals. The first term of eq. (10) exhibits a huge enhancement at the critical valence transition point where $|(\partial n_f/\partial \epsilon_f)_\mu|$ diverges. This huge enhancement should be compared to the moderate enhancement around the magnetic quantum critical point where the enhancement arises only through the renormalization amplitude z , as discussed in ref. 35.

5. CeCu₂Si₂

The first heavy fermion superconductor to be discovered, CeCu₂Si₂, is the archetypical ‘potato’. It has a very irregularly shaped superconducting region under pressure, with a large enhancement of T_c at around 3 GPa, well away from the antiferromagnetic QCP, which is thought to be at a small positive pressure p_c of approximately 0.1 GPa.³⁶⁾ CeCu₂Si₂ has been the subject of intensive study by the authors, in which we showed that the enhancement of T_c under pressure was linked to a sharp Ce valence transition.^{8, 37–42)}

The link between superconductivity and valence change had been noted by Jaccard and coworkers since the first measurements of CeCu₂Si₂ under high pressure in 1984.⁴³⁾ The isostructural sister compound CeCu₂Ge₂ was shown to behave in a very similar way, with a shift of around 10 GPa corresponding to the larger atomic size of Ge.^{9, 44)}

Strong evidence for a sharp valence transition in CeCu₂Ge₂ was presented by Vargoz *et al.*^{9, 45)} They showed that the A coefficient of a Fermi-liquid fit to the resistivity $\rho = \rho_0 + AT^2$, when plotted against the low-temperature maximum in resistivity T_1^{max} showed the expected relationship $A \propto (T_1^{\text{max}})^{-2}$ in two regions, with a rapid crossover between them. As $T_1^{\text{max}} \propto T_K \propto \gamma^{-1}$, where γ is the electronic specific heat coefficient, this corresponds to a crossover from the strongly correlated to weakly correlated branch of the Kadowaki-Woods plot.³⁰⁾ The maximum in T_c seemed to correspond to the position of this crossover.

Motivated by these results, and by theoretical predictions by Miyake and coworkers,^{1, 46)} we (ATH and DJ) carried out detailed measurements of resistivity and specific heat (by the ac calorimetry method) on a single crystal sample of CeCu₂Si₂ in a solid helium pressure medium up to nearly 7 GPa.⁸⁾ The use of helium ensures

the most hydrostatic possible conditions at low temperature, a feature of crucial importance given the rapidly changing behaviour of CeCu_2Si_2 with pressure. Simultaneous measurements of resistivity and specific heat enabled us to verify the bulk nature of the superconductivity in the high pressure region, and identify the most reliable criterion for defining T_c .

We identified a pressure P_v , at about 4.5 GPa, which corresponds to a valence critical pressure. Around this point there are a series of anomalies associated with a delocalisation of the Ce 4f electron. P_v is slightly above the pressure where T_c reaches a maximum, according to both the theoretical prediction and our observations.

5.1 Indications of a Valence Instability

The drastic decrease of the A coefficient of resistivity, and its change of scaling with respect to $(T_1^{\max})^{-2}$ are clear signs of the transition from a strongly correlated to weakly correlated regime. Table II shows the complete list of anomalies found around the valence instability in CeCu_2Si_2 and CeCu_2Ge_2 . Fig. 7 shows how the enhancement of T_c , and the anomalies in ρ_0 and γ correspond to the change from a strongly to weakly correlated regime.

5.2 $\text{CeCu}_2(\text{Si}_{1-x}\text{Ge}_x)_2$

The existence of a second quantum critical point at high pressure in CeCu_2Si_2 was given further backing by Yuan *et al.*⁵⁶⁾ They doped the pure CeCu_2Si_2 system with Ge (effectively applying negative pressure and introducing disorder) and then applied pressure to come back along the pressure/volume axis. For increasing proportions of Ge, the superconductivity was weakened, and for large enough x the superconducting region could be split into two domes, near P_c and P_v respectively.

5.3 Valence fluctuation mediated superconductivity in CeCu_2Si_2

Figure 8 shows the pressure variation of the superconducting transition temperature in CeCu_2Si_2 determined by specific heat and resistivity. It is clear from this, and Fig. 9, that the bulk transition temperature determined from the specific heat coincides with the point at which the resistance reaches zero. Over a large pressure range the resistive transitions are very broad. This is often attributed to pressure gradients in the cell; in this case, however, as a helium medium was used the gradients should be negligible.

The nature of the broad resistive transitions was investigated in detail at 1.78 GPa as a function of measurement current and magnetic field, as shown in Figs. 10 and 11. Remarkably, the high temperature part of the resistance drop disappears completely as the current is increased, recovering a sharp transition. Applying a magnetic field has the opposite effect; the low temperature part of the transition is rapidly suppressed with field, while the upper part remains up to much higher fields. There appear to be two distinct transitions, with different T_c 's and hence critical fields. The current dependence implies that the 'high T_c ' superconductivity is of a filamentary nature, so its critical current density is easily exceeded. We should note that even the best samples,

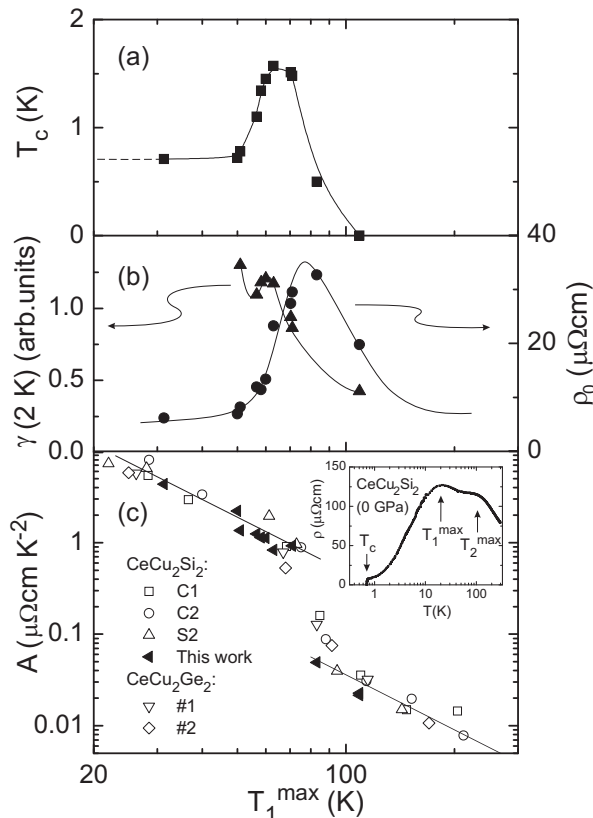


Fig. 7. Plotted against T_1^{\max} (defined in inset), a measure of the characteristic energy scale of the system, are (a) the bulk superconducting transition temperature, (b) the residual resistivity and estimate $\tilde{\gamma}$ of the Sommerfeld coefficient, and (c) the coefficient A of the $\rho \sim AT^2$ law of resistivity, including data from CeCu_2Ge_2 . Note the straight lines where the expected $A \propto (T_1^{\max})^{-2}$ scaling is followed. The maximum of T_c coincides with the start of the region where the scaling relation is broken, while the maximum in residual resistivity is situated in the middle of the collapse in A . Pressure increases towards the right-hand side of the scale (high T_1^{\max}). After ref. 8.

with the highest values of T_c , showed very broad resistive transitions at certain pressures.

The enhancement of the residual resistivity at P_v will be discussed in more detail below, but it reveals another remarkable feature of the high pressure superconductivity in CeCu_2Si_2 . In certain samples of CeCu_2Si_2 , the residual resistivity, while relatively large at ambient pressure, reaches enormous values approaching the Ioffe-Regel limit around P_v , i.e. the mean free path is of the order of the lattice spacing.

Magnetically mediated superconductors such as CePd_2Si_2 are notoriously dependent on sample quality, superconductivity only appearing in the purest samples with very small values of ρ_0 , of the order of a few $\mu\Omega\text{cm}$. Fig. 12 shows two CeCu_2Si_2 samples with very different residual resistivities, in which a nearly complete resistive transition can be seen at 4.34 GPa despite a residual resistivity of nearly $200 \mu\Omega\text{cm}$ around P_v . This is probably the most compelling evidence for a new mechanism of superconductivity at high pressure in CeCu_2Si_2 .

The superconducting transition temperature and pressure range is highly sensitive to small uniaxial stresses.

Table II. Anomalies in CeCu_2Si_2 and CeCu_2Ge_2 associated with valence transition, with references. Symbols explained in the text.

Part (i): Direct evidence for sudden valence change.

Part (ii): Anomalies explained theoretically by the GPAM^{1, 8, 34} (§4).

Part (iii): Other anomalies observed around crossover to intermediate valence with pressure.

| | CeCu_2Si_2 | CeCu_2Ge_2 |
|---|----------------------------|----------------------------|
| | Ref. | Ref. |
| Volume discontinuity | - | 47 |
| (i) L_{III} X-ray absorption | 48 | - |
| Drastic change of A by two orders of magnitude | 8,9 | 9 |
| Change of $A \propto (T_1^{\text{max}})^{-2}$ scaling | 8,9 | 9 |
| Maximum in $T_c(P)$ | 8,43 | 49 |
| (ii) Large peak in ρ_0 | 8,9 | 9 |
| Maximum in $\gamma \simeq (C_P/T)$ | 8,50 | - |
| $\rho \propto T^n$ from $T_c < T < T^*$, with $n(P_V) = 1$ minimum | 8,43,51 | 9 |
| Sample dependence of T_c | 8,9,40,43,45,52-54 | 9 |
| (iii) Enhanced $\left. \frac{\Delta C_P}{\gamma T} \right _{T_c}$ | 8 | - |
| Resistivity and thermopower indicate $T_1^{\text{max}} \simeq T_2^{\text{max}}$ | 9,51 | 9,55 |
| Broad superconducting transition widths ΔT_c | 8,40,43 | 9 |

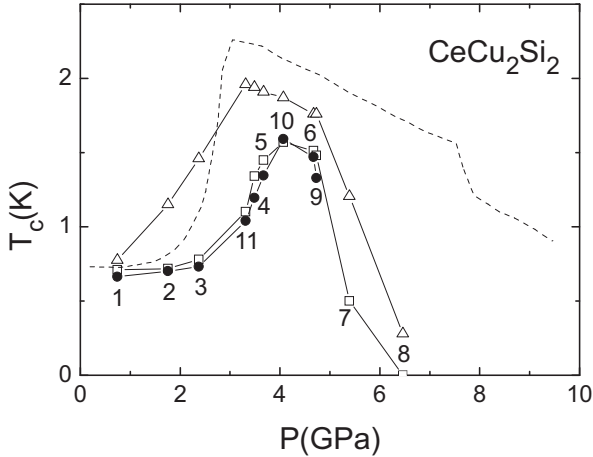


Fig. 8. $T_c(P)$ in CeCu_2Si_2 determined from resistivity and specific heat measurements. The triangles show T_c determined from the onset of the resistive transition (T_c^{onset}), the squares show its completion ($T_c^{R=0}$), and the filled circles show the midpoint of the specific heat jump. The numbers indicate the sequence of pressures. The dotted line shows T_c determined by susceptibility in a different sample, also in a helium pressure medium.⁵² After ref. 8.

We investigated this effect by placing single crystal samples from neighbouring positions on the same source crystal in a Bridgman anvil cell with their tetragonal c -axis parallel and perpendicular to the force loading direction. As this technique uses a solid steatite pressure medium, there remains some non-hydrostatic component to the stress inside the cell, which can be exploited as a qualitative control parameter. We showed³⁹) that there is a significant difference in T_c between the two orientations, and that P_V is shifted to a higher pressure in the case where the force loading direction is perpendicular to the c -axis. This shows from an experimental point of view that any considerations related to the anisotropy of a

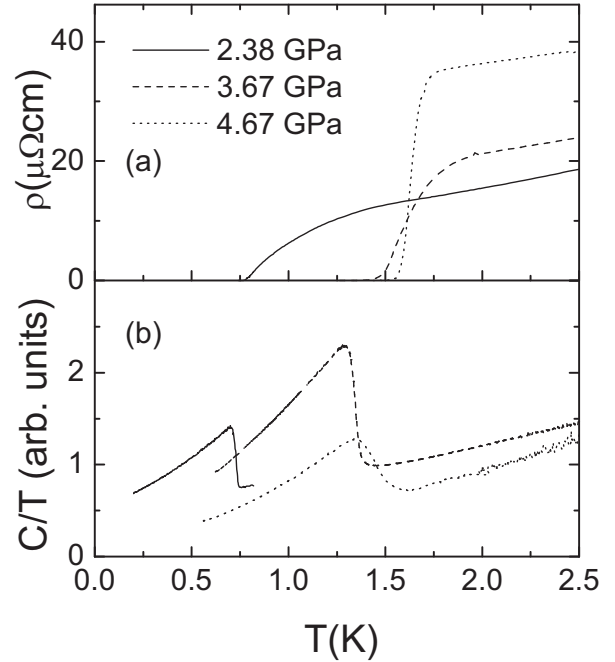


Fig. 9. Superconducting transition at three pressures in (a) resistivity and (b) specific heat. Note the width of the resistive transitions, and the fact that the start of the jump in specific heat coincides with the completion of the resistive transition. After ref. 8

system must also be taken into account in the case of CVF-mediated superconductivity.

5.4 Normal state properties of CeCu_2Si_2 around P_V

Three key properties of the normal state in CeCu_2Si_2 show characteristic behaviour at the valence instability P_V : the residual resistivity ρ_0 , the power-law behaviour of the T -dependence of the resistivity, and the Sommerfeld coefficient of the electronic specific heat capacity γ .

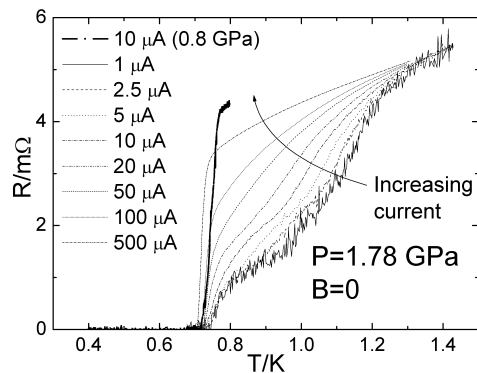


Fig. 10. At 1.78 GPa, the resistive transition in CeCu_2Si_2 is very broad, and appears to have two distinct resistance drops. By increasing the measurement current, the upper part of the transition is suppressed, and a sharp transition comparable to that close to ambient pressure is recovered. Note that the pressure gradient is negligible, so the broad transitions are intrinsic to the sample.

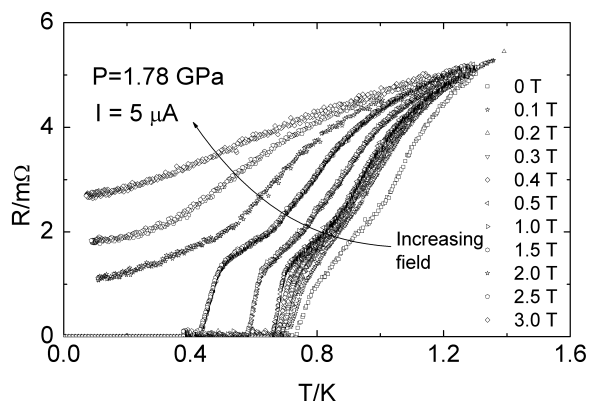


Fig. 11. By applying a magnetic field, the lower part of the resistive transition is suppressed more rapidly than the upper part.

These will be discussed in the next section.

A key prediction of the GPAM is the enhancement of impurity scattering around the valence instability discussed in §4.3. This can be thought of as an impurity nucleating a change of valence in the Ce atoms surrounding it, thereby inflating its scattering cross-section, and hence the residual resistivity, as given by eq. (10).

Fig. 13 shows the pressure dependence of ρ_0 in a number of different CeCu_2Si_2 samples, which can all be scaled on to the same Lorentzian curve by a simple linear transformation. This scaling behavior of ρ_0 would be possible if the universal form is given by $\ln |(-\partial n_\epsilon / \partial \epsilon_\epsilon)_\mu / N_F|$.

It should be noted that the impurity contribution to the resistivity has a negative temperature dependence, a fact especially evident at very high pressure where the A -coefficient of the resistivity becomes small. Even in samples with a small ρ_0 this can cause problems when fitting power laws to the resistivity in the region above P_V .

Due to the localised nature of the critical valence fluctuations, the quasiparticle scattering is nearly q -

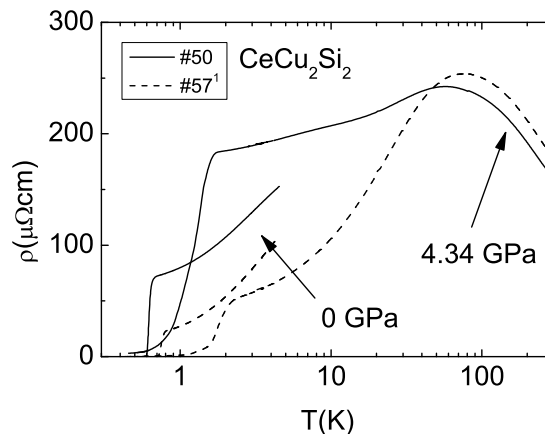


Fig. 12. Resistivity at ambient pressure and close to P_V of two polycrystalline CeCu_2Si_2 samples prepared by Ishikawa. Note the large increase in residual resistivity under pressure combined with a nearly complete resistive transition. After ref. 41

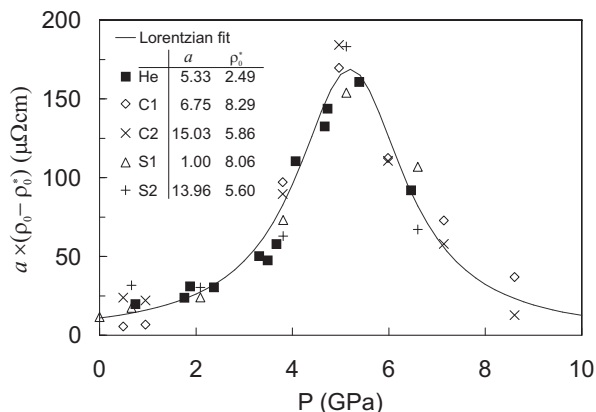


Fig. 13. Enhancement of residual resistivity in several different CeCu_2Si_2 samples, scaled to a universal pressure dependence, with a and ρ_0^0 being normalizing factors. The maximum in ρ_0 is at a pressure slightly higher than that corresponding to the maximum in T_c . After ref. 8.

independent, leading to a linear resistivity, implied by eq. (7). Fig. 14 shows the resistivity at a pressure very close to P_V , where a strictly linear temperature dependence is observed over a broad temperature range.

The electronic specific heat coefficient γ , and hence the effective mass m^*/m , can be estimated by following the calorimetric signal C/T , at a fixed temperature and measurement frequency above the superconducting transition, though this includes constant or slowly varying addenda from the helium, diamonds etc. Figure 15 shows the estimate $\tilde{\gamma}(P)$, along with the value deduced from measurements of the upper critical field.⁵⁰⁾ A single constant scale factor has been introduced, showing that the two curves can be superimposed. There is a clear anomaly in $\tilde{\gamma}$ at 4 GPa (just below the pressure corresponding to T_c^{max}), superimposed on a constant reduction with pressure. The effective mass is also reflected in the initial slope of the upper critical field $H_{c2}'(T_c)$, which in our sample also had a maximum at the same pressure

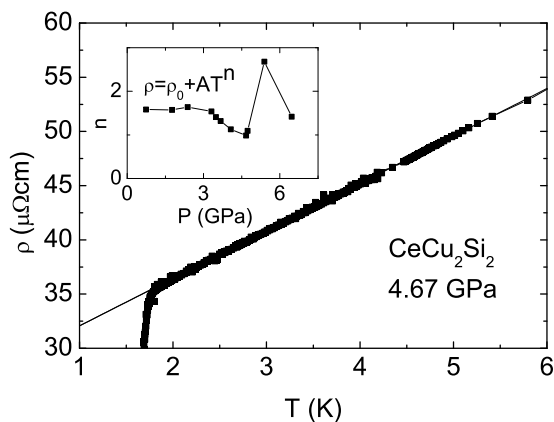


Fig. 14. Linear resistivity $\rho - \rho_0 \propto T$ is found over a broad temperature range at pressures close to P_v . The inset shows the result of a power law fit at different pressures between T_c and 4.2 K.

as the peak in $\tilde{\gamma}$. Equation (8) implies an enhancement of γ at P_v due to critical valence fluctuations; combined with a monotonic reduction in effective mass due to the rapid change of n_f with pressure, this leads to a peak in γ observed slightly below P_v .

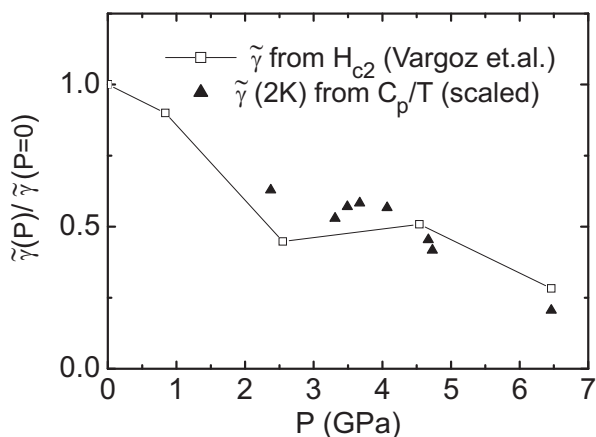


Fig. 15. Estimate $\tilde{\gamma}(P)$ of the Sommerfeld coefficient from a.c.-calorimetry signal at 2 K (triangles), scaled for comparison with that deduced from H_{c2} measurements (squares).⁵⁰⁾ The noise on the calorimetry signal is smaller than the symbol size, however see ref. 8 for a discussion of possible systematic errors.

6. Other Candidates for Critical Valence Fluctuation Mediated SC

After CeCu_2Si_2 and CeCu_2Ge_2 , the next strongest candidates for CVF mediated superconductivity are probably the Ce115 compounds. Between them they show a number of the properties discussed above, namely linear resistivity in CeCoIn_5 ,⁵⁷⁾ and linear resistivity and a pressure-induced maximum of ρ_0 in CeRhIn_5 .^{58, 59)}

CeIrIn_5 is probably the strongest candidate for a CVF mediated superconductor at ambient pressure. Pressure studies on $\text{CeRh}_{1-x}\text{Ir}_x\text{In}_5$ have showed that the superconducting region can be split into two distinct pockets,

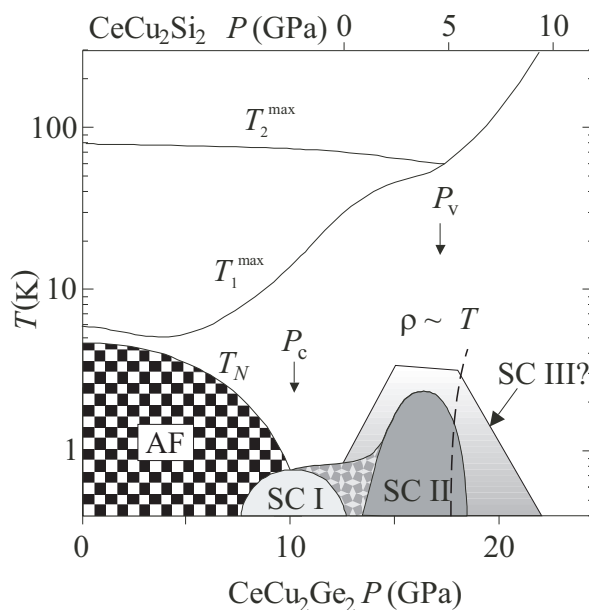


Fig. 16. Schematic P - T phase diagram for $\text{CeCu}_2(\text{Si/Ge})_2$ showing the two critical pressures P_c and P_v . At P_c , where the antiferromagnetic ordering temperature $T_N \rightarrow 0$, superconductivity in region $SC I$ is mediated by antiferromagnetic spin fluctuations; around P_v , in the region $SC II$, valence fluctuations provide the pairing mechanism and the resistivity is linear in temperature. The temperatures T_1^{\max} , and T_2^{\max} , merge at a pressure coinciding with P_v . The dashed line represents a hypothetical (weakly) first order valence transition with a critical end point close to zero temperature.

with a cusp-like minimum of T_c at around $x = 0.9$.⁶⁰⁾ ¹¹⁵In-NQR measurements of stoichiometric CeIrIn_5 under pressure showed that while T_c increased under pressure, reaching $T_c^{\max} \simeq 1$ K at 3 GPa, more than twice its value at ambient pressure, the nuclear-spin-lattice-relaxation rate ($1/T_1$) was found to decrease monotonically with pressure. This indicates that the antiferromagnetic spin fluctuations are *decreasing* with pressure, while the superconductivity is strengthening.

The cases of PuCoGa_5 ⁶¹⁾ and PuRhGa_5 ⁶²⁾ are also very intriguing. They become superconducting at the comparatively high temperatures of 18 K and 9 K respectively. Pu metal itself has very rich phase diagram whose origin may be traced back to the fact that the 5f electrons in Pu are located near the boundary between the localized state with nearly an integral valence and the itinerant state with a fractional valence. There exists some circumstantial evidence to support the possibility of CVF-mediated superconductivity in these compounds. The ratio A/γ^2 of the Pu115 compounds ($A/\gamma \sim 2 \times 10^{-6} [\mu\Omega\text{cm mol}^2\text{K}^2/\text{J}^2]$ for PuCoGa_5 ⁶³⁾) lies between that of strongly and weakly correlated metals. This suggests that Pu115 compounds are not strongly correlated metals but depend on the valence fluctuations of the Pu ion, although the Sommerfeld coefficient $\gamma \sim 95 [\text{mJ}/\text{K}^2\text{mol}]$ is moderately enhanced.

There are other examples among the ‘potato’ compounds mentioned above, such as the two separate domes of superconductivity in the phase diagram of CeNi_2Ge_2 , and broad resistive transitions and apparent enhance-

ment of ρ_0 under pressure in CeNiGe₃, but these have not been studied in so much detail.

In CeCu₂Si₂ and CeCu₂Ge₂ the two critical pressures P_V and P_C corresponding to the magnetic and valence instabilities are well separated. It may be the case in other systems, however, that $P_V \sim P_C$, or even $P_V < P_C$. There is a clear need for some sort of ‘smoking gun’ to distinguish between valence and magnetically mediated superconductivity. Both are predicted to be *d*-wave, but knowledge of the precise gap symmetry, though very difficult to determine under pressure, may be the key to distinguishing these two mechanism.

7. Conclusions

Ce metal and a small number of its compounds show a first order valence transition in their pressure-temperature phase diagrams. We contend that an analogous first-order or nearly first order transition is present in many Ce compounds, and in certain circumstances, fluctuations around its critical end point can mediate superconductivity.

CeCu₂Si₂ has been shown almost unambiguously to have a region of superconductivity at high pressure mediated by such critical valence fluctuations, close to a valence instability at a pressure around 4.5 GPa. There are a number of anomalies in the normal state around this pressure which can be tied to an abrupt delocalisation of the Ce 4f electron.

A majority of the other known Ce-based HF superconductors have characteristics which cannot be explained purely in a spin fluctuation mediated scenario. The presence of a valence instability in these compounds may be quite general, and the key to a more complete understanding of their behaviour.

Acknowledgment

This work was supported by a Grant-in-Aid for Creative Scientific Research (15GS0213), a Grant-in-Aid for Scientific Research (Nos. 16340103 & 15204032), and the 21st Century COE Program (G18) by the Japan Society for the Promotion of Science.

References

- 1) Y. Onishi and K. Miyake: J. Phys. Soc. Jpn. **69** (2000) 3955.
- 2) A. Demuer, A. T. Holmes and D. Jaccard: J. Phys: Condens. Matter **14** (2002) L529.
- 3) M. Nicklas, R. Borth, E. Lengyel, P. G. Pagliuso, J. L. Sarrao, V. A. Sidorov, G. Sparn, F. Steglich and J. D. Thompson: J. Phys: Condens. Matter **13** (2001) L905.
- 4) P. Monthoux and G. G. Lonzarich: Phys. Rev. B **59** (1999) 14598.
- 5) P. Monthoux and G. G. Lonzarich: Phys. Rev. B **63** (2001) 054529.
- 6) P. Monthoux and G. G. Lonzarich: Phys. Rev. B **69** (2004) 064517.
- 7) N. D. Mathur, F. M. Grosche, S. R. Julian, I. R. Walker, D. M. Freye, R. K. W. Haselwimmer and G. G. Lonzarich: Nature **394** (1998) 39.
- 8) A. T. Holmes, D. Jaccard and K. Miyake: Phys. Rev. B **69** (2004) 024508.
- 9) D. Jaccard, H. Wilhelm, K. Alami-Yadri and E. Vargoz: Physica B **259–261** (1999) 1.

- 10) F. M. Grosche, P. Agarwal, S. R. Julian, N. J. Wilson, R. K. W. Haselwimmer, S. J. S. Lister, N. D. Mathur, F. V. Carter, S. S. Saxena and G. G. Lonzarich: J. Phys: Condens. Matter **12** (2000) L533.
- 11) R. Movshovich, T. Graf, D. Mandrus, J. D. Thompson, J. L. Smith and Z. Fisk: Phys. Rev. B **53** (1996) 8241.
- 12) H. Wilhelm, S. Raymond, D. Jaccard, O. Stockert, H. v. Loehneysen and A. Rosch: in *Proc. AIRAPT-17, Hawaii, 1999* ed. M. Manghnani, W. Nellis and M. Nicol (Universities Press, Hyderabad, 2000) p. 697.
- 13) V. A. Sidorov, M. Nicklas, P. G. Pagliuso, J. L. Sarrao, Y. Bang, A. V. Balatsky and J. D. Thompson: Phys. Rev. Lett. **89** (2002) 157004.
- 14) T. Muramatsu, T. C. Kobayashi, K. Shimizu, K. Amaya, D. Aoki, Y. Haga and Y. Onuki: Physica C **388–389** (2003) 539.
- 15) E. Vargoza, P. Link, D. Jaccard, T. L. Bihan and S. Heathman: Physica B **229** (1996) 225.
- 16) M. Nicklas, V. A. Sidorov, H. A. Borges, P. G. Pagliuso, C. Petrovic, Z. Fisk, J. L. Sarrao and J. D. Thompson: Physical Review B (Condensed Matter and Materials Physics) **67** (2003) 020506.
- 17) H. Kotegawa, T. Miyoshi, K. Takeda, S. Fukushima, H. Hidaka, K. Tabata, T. C. Kobayashi, M. Nakashima, A. Thamizhavel, R. Settai and Y. Onuki: Physica B **378** (2006) 419.
- 18) M. Nicklas, G. Sparn, R. Lackner, E. Bauer and F. Steglich: Physica B **359** (2005) 386.
- 19) N. Kimura, K. Ito, K. Saitoh, Y. Umeda, H. Aoki and T. Terashima: Phys. Rev. Lett. **95** (2005) 247004.
- 20) I. Sugitani, Y. Okuda, H. Shishido, T. Yamada, A. Thamizhavel, E. Yamamoto, T. D. Matsuda, Y. Haga, T. Takeuchi, R. Settai and Y. Onuki: J. Phys. Soc. Jpn. **75** (2006) 3703.
- 21) K. Kadowaki and S. Woods: Solid State Commun. **58** (1986) 507.
- 22) D. G. Koskenmaki and K. A. Gschneidner, Jr.: in *Handbook on the Physics and Chemistry of Rare Earths*, edited by K. A. Gschneidner, Jr. and L. Eyring (North-Holland, Amsterdam, 1979), Vol. I, p. 337.
- 23) D. Gignoux and J. Voiron: Phys. Rev. B **32** (1985) 4822.
- 24) A. Jayaraman, W. Lowe, L. D. Longinotti and E. Bucher: Phys. Rev. Lett. **36** (1976) 366.
- 25) S. M. Shapiro, J. D. Axe, R. J. Birgeneau, J. M. Lawrence and R. D. Parks: Phys. Rev. B **16** (1977) 2225.
- 26) E. Gaudin, B. Chevalier, B. Heying, U. Rodewald and R. Pottgen: Chem. of Mater. **17** (2005) 2693.
- 27) A. Svane, P. Strange, W. Temmerman, Z. Szotek, H. Winter and L. Petit: Phys. Stat. Sol. (b) **223** (2001) 105.
- 28) T. M. Rice and K. Ueda: Phys. Rev. B **34** (1986) 6420.
- 29) H. Shiba: J. Phys. Soc. Jpn. **55** (1986) 2765.
- 30) K. Miyake, T. Matsuura and C. M. Varma: Solid State Commun. **71** (1989) 1149.
- 31) Y. Onishi and K. Miyake: Physica B **281–282** (2000) 191.
- 32) K. Miyake, S. Schmitt-Rink and C. M. Varma: Phys. Rev. B **34** (1986) 6554.
- 33) S. Watanabe, M. Imada and K. Miyake: Journal of the Physical Society of Japan **75** (2006) 3710.
- 34) K. Miyake and H. Maebashi: J. Phys. Soc. Jpn. **71** (2002) 1007.
- 35) K. Miyake and O. Narikiyo: J. Phys. Soc. Jpn. **71** (2002) 867.
- 36) P. Gegenwart, C. Langhammer, C. Geibel, R. Helfrich, M. Lang, G. Sparn, F. Steglich, R. Horn, L. Donnevert, A. Link and W. Assmus: Phys. Rev. Lett. **81** (1998) 1501.
- 37) A. T. Holmes, A. Demuer and D. Jaccard: Acta Phys. Pol., B **34** (2003) 567.
- 38) D. Jaccard and A. T. Holmes: Physica B **359–361** (2005) 333.
- 39) D. Jaccard and A. T. Holmes: Physica B **359** (2005) 333.
- 40) A. T. Holmes, D. Jaccard, H. S. Jeevan, C. Geibel and M. Ishikawa: J. Phys: Condens. Matter **17** (2005) 5423.
- 41) A. T. Holmes and D. Jaccard: Physica B Condensed Matter **378** (2006) 339.
- 42) A. T. Holmes: Dr. Thesis, University of Geneva, no. 3539, Geneva 2004.

- <http://www.unige.ch/cyberdocuments/theses2004/HolmesAT/these.pdf>
- 43) B. Bellarbi, A. Benoit, D. Jaccard, J. M. Mignot and H. F. Braun: Phys. Rev. B **30** (1984) 1182.
- 44) D. Jaccard, P. Link, E. Vargoz and K. Alami-Yadri: Physica B **230–232** (1997) 297.
- 45) E. Vargoz: Dr. Thesis, University of Geneva, no. 3003, Geneva 1998.
- 46) K. Miyake, O. Narikiyo and Y. Onishi: Physica B **259–261** (1999) 676.
- 47) A. Onodera, S. Tsuduki, Y. Ohishi, T. Watanuki, K. Ishida, Y. Kitaoka and Y. Onuki: Solid State Commun. **123** (2002) 113.
- 48) J. Roehler, J. Klug and K. Keulerz: J. Magn. Magn. Mater. **76–77** (1988) 340.
- 49) E. Vargoz and D. Jaccard: J. Magn. Magn. Mater. **177–181** (1998) 294.
- 50) E. Vargoz, D. Jaccard, J. Y. Genoud, J. P. Brison and J. Flouquet: Solid State Commun. **106** (1998) 631.
- 51) D. Jaccard, J. M. Mignot, B. Bellarbi, A. Benoit, H. F. Braun and J. Sierro: J. Magn. Magn. Mater. **47–48** (1985) 23.
- 52) F. Thomas, C. Ayache, I. A. Fomine, J. Thomasson and C. Geibel: J. Phys: Condens. Matter **8** (1996) L51.
- 53) J. Thomasson, Y. Okayama, I. Sheikin, J. P. Brison and D. Braithwaite: Solid State Commun. **106** (1998) 637.
- 54) D. Jaccard, E. Vargoz, K. Alami-Yadri and H. Wilhelm: Rev. High Pressure Sci. Techno. **7** (1998) 412.
- 55) P. Link, D. Jaccard and P. Lejay: Physica B **225** (1996) 207.
- 56) H. Q. Yuan, M. Deppe, G. Sparrn, C. Geibel and F. Steglich: Acta Phys. Pol., B **34** (2003) 533.
- 57) C. Petrovic, P. G. Pagliuso, M. F. Hundley, R. Movshovich, J. L. Sarrao, J. D. Thompson, Z. Fisk and P. Monthoux: J. Phys: Condens. Matter **13** (2001) L337.
- 58) H. Hegger, C. Petrovic, E. G. Moshopoulou, M. F. Hundley, J. L. Sarrao, Z. Fisk and J. D. Thompson: Phys. Rev. Lett. **84** (2000) 4986.
- 59) T. Muramatsu, N. Tateiwa, T. C. Kobayashi, K. Shimizu, K. Amaya, D. Aoki, H. Shishido, Y. Haga and Y. Onuki: J. Phys. Soc. Jpn. **70** (2001) 3362.
- 60) M. Nicklas, V. A. Sidorov, H. A. Borges, P. G. Pagliuso, J. L. Sarrao and J. D. Thompson: Phys. Rev. B **70** (2004) 020505.
- 61) J. L. Sarrao, L. A. Morales, J. D. Thompson, B. L. Scott, G. R. Stewart, F. Wastin, J. Rebizant, P. Boulet, E. Colineau and G. H. Lander: Nature **420** (2002) 297.
- 62) F. Wastin, P. Boulet, J. Rebizant, E. Colineau and G. H. Lander: J. Phys: Condens. Matter **15** (2003) S2279.
- 63) F. Wastin: Private communication.